Journal of Electromagnetic Waves and Applications, Vol. 14, 185–203, 2000

SAR INTERFEROMETRIC COHERENCE IN WIDE BAND SYSTEMS

L. Sagués, M. Bara, X. Fàbregas, and A. Broquetas

Dpt. Teoria del Senyali Comunicacions
Universitat Politècnica de Catalunya (UPC)
Campus Nord UPC, D3
c/ Jordi Girona, 1–3
08034 Barcelona, Spain

Abstract–This paper presents a study of the interferometric coherence aimed to the understanding of the main sources of phase error of an operative wide band system. This objective is accomplished by finding a theoretical expression of coherence based on a suitable model capable of including the roughness of the surface, which produces decorrelation besides the conventional spectral overlapping approach. The analysis is validated by means of numerical simulations and controlled experiments in anechoic chamber, with the aim of extrapolating the obtained results to airborne and spaceborne imaging radars.

1. INTRODUCTION

One of the applications of SAR Interferometry is the generation of topographic maps by means of combining two complex SAR images from slightly different viewing angles [1]. Future airborne and spaceborne interferometric SAR systems are planed to use a wide frequency bandwidth, appropriate for the production of very high resolution Digital Elevation Models (DEM). Wide band systems also present other benefits such the possibility of combining different bands to ease the phase unwrapping process, or removing atmospheric effects at lower frequencies. Although large bandwidth sensors are not available yet in the current airborne and satellite SAR platforms, present ground-based systems can work with a wide range of frequencies by using a continuous wave stepped frequency sweep. This is the case of an ultra wide band scatterometer developed in the Universitat Politècnica

de Catalunya (Barcelona–Spain) [2]. This scatterometer can operate as an imaging system by forcing the antennas to describe a circular trajectory around a rotating vertical mast [3]. This imaging system also offers the possibility of carrying out interferometric measurements by changing the position of the antennas [4]. Such an instrument provides an excellent tool to study and validate interferometry applications and to anticipate possible problems related to future wide band spaceborne systems. The paper shows the results of several experiments carried out in anechoic chamber in order to obtain a height profile from a metallic rough surface. The interferometric coherence values obtained experimentally are compared with the predicted coherence from the spatial baseline decorrelation analysis [5] and numerical simulations on a random surface.

The remainder of the paper is organized as follows. An interferometric coherence expression which takes into account the impact of the surface roughness is obtained in Section 2. In this section we also give a new critical baseline criterion considering the volumetric effects besides the well-known spatial baseline decorrelation. In Section 3, some simulated and experimental results are presented and compared with those predicted from the theoretical expression obtained in Section 2. We close, in Section 4, with the summary and conclusions.

2. INTERFEROMETRIC COHERENCE EXPRESSION FOR ROUGH SURFACES

The geometry of an interferometric imaging system is illustrated in Figure 1. The interferogram is formed by cross-multiplying two SAR images from slightly different viewing angles. The antennas are located at two different positions A_1 and A_2, illuminating the same patch on the surface at two incidence angles θ_1 and θ_2, respectively. The distance between the two antenna positions is known as the baseline distance B, whereas the baseline projection normal to the look direction is called B_n. The distance from each antenna to the center of the resolution cell is r. The cross range (azimuth) distance is x and the ground range distance is y. For simplicity, let us assume that the problem is non-variant in the cross range dimension, and the resolution cell of the rough surface is formed by N non-directional independent scatterers uniformly distributed along the y-axis. Each scatterer is characterized by the height random process h_n, measured with respect to $z = 0$. The complex value of the field scattered back to the

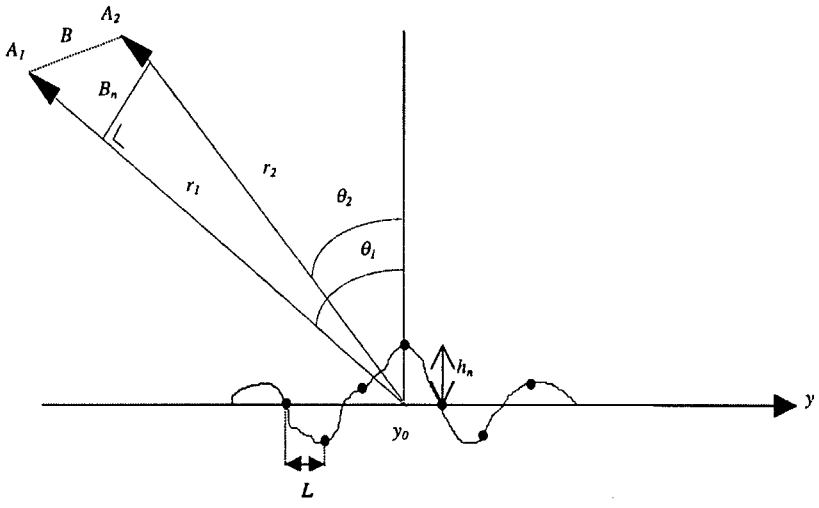

Figure 1. Interferometric SAR geometry.

receiver will be given by the coherent addition of the contributions associated with each scatterer:

$$E_s(f,\theta_i) = |E_0| \cdot \frac{e^{-j\frac{4\pi}{c}fr}}{r^2} \sum_n S_n \cdot e^{-j\frac{4\pi}{c}f(nL\sin\theta_i - h_n\cos\theta_i)} \tag{1}$$

where θ_i $(i = 1 \text{ or } 2)$ is the viewing angle from each antenna position, n is the index of scatterers, L is their ground separation and S_n their reflectivity. The argument of the exponential term indicates the wave path to each scatterer, while E_0 is a constant that depends, among others, on parameters of the system such as antenna gain and transmitted power. If we assume that a continuous wave stepped frequency scan is used in order to achieve a wide bandwidth W and that the C-SAR reconstruction algorithm is applied, then the signal measured in the final processed image at position y_0 can be expressed as the Inverse Fourier Transform of Eq. (1):

$$s(\theta_i) = |E_0| \cdot \frac{W}{r^2} \sum_n S_n \cdot \sin c\left[(nL\sin\theta_i - h_n\cos\theta_i)/R_s\right] e^{-j\frac{4\pi}{c}f_0(nL\sin\theta_i - h_n\cos\theta_i)} \tag{2}$$

where R_s is the slant range resolution and f_0 is the center frequency of the used frequency range. Therefore, the cross-correlation of the two signals $s(\theta_1)$ and $s(\theta_2)$, from which we determine the interferometric phase, will be:

$$\begin{aligned} s(\theta_1)\cdot s(\theta_2)^* = |E_0|^2 \cdot \frac{W^2}{r_1^2 r_2^2} \sum_n \sum_{n'} S_n \\ \cdot S_{n'}^* \operatorname{sin} c\left[(nL\sin\theta_1 - h_n\cos\theta_1)/R_s\right] \\ \cdot \operatorname{sin} c\left[(n'L\sin\theta_2 - h_{n'}\cos\theta_2)/R_s\right] \\ \cdot e^{-j\frac{4\pi}{c}f_0(nL\sin\theta_1 - h_n\cos\theta_1)} \\ \cdot e^{+j\frac{4\pi}{c}f_0(n'L\sin\theta_2 - h_{n'}\cos\theta_2)} \end{aligned} \tag{3}$$

The coherence between both signals can be obtained by applying the expectation operator to Eq. (3). If we take into consideration that the difference in viewing angles is small, and the scatterers are uncorrelated $\left(\langle S_n . S_{n'}^*\rangle = \sigma_s^2 \delta_{n,n'}\right)$, then Eq. (3) can be approximated by:

$$\begin{aligned} \langle s(\theta_1)\cdot s(\theta_2)^*\rangle \approx C \sum_n \Big\langle \operatorname{sin} c^2\left((nL\sin\theta - h_n\cos\theta)/R_s\right) \\ \cdot e^{-j\frac{4\pi}{c}f_0 h_n(\cos\theta_2 - \cos\theta_1)}\Big\rangle \\ \cdot e^{-j\frac{4\pi}{c}f_0 nL(\sin\theta_1 - \sin\theta_2)} \end{aligned} \tag{4}$$

where θ is the average look angle and C an arbitrary complex constant. Both $\operatorname{sin} c$ functions are considered to have the same argument since in most practical cases the difference in incidence angles is small. If the variance of the random variable h_n is also small compared to the width R_s of the $\operatorname{sin} c$ function, then it is possible to take into account its effect only on the exponential factor:

$$\begin{aligned} \langle s(\theta_1)\cdot s(\theta_2)^*\rangle \approx C \sum_n \operatorname{sin} c^2(nL\sin\theta/R_s) \cdot \left\langle e^{-j\frac{4\pi}{c}f_0 h_n(\cos\theta_2 - \cos\theta_1)}\right\rangle \\ \cdot e^{-j\frac{4\pi}{c}f_0 nL(\sin\theta_1 - \sin\theta_2)} \end{aligned} \tag{5}$$

The validity of this assumption is discussed in Section 3 by means of numerical simulations. The statistic term of Eq. (5) can be computed considering that the random variable h_n is characterized by

a zero-mean gaussian distribution, which is an appropriate model for rough surfaces [5]. The deterministic term corresponds to the Discrete Fourier Transform of a squared sinc, which is a triangular function. Therefore, after the normalization of Eq. (5), we obtain the interferometric coherence between the two signals from a single resolution cell. It can be expressed approximately as the multiplication of two terms, each of them related to two different sources of decorrelation:

$$\gamma \approx \left[1 - \frac{|\sin\theta_1 - \sin\theta_2|}{\sin\theta} \cdot \frac{f_0}{W}\right] \cdot \left[e^{-2\left(\frac{2\pi}{c} f_0 (\cos\theta_2 - \cos\theta_1)\right)^2 \cdot {\sigma_h}^2}\right] \qquad (6)$$

where ${\sigma_h}^2$ is the variance of the process h_n. It is important to note that this new expression includes the effect of the surface roughness (by means of which we can model the so-called *volumetric effects*).

The first term relates to the well-known spatial baseline decorrelation, which basically depends on the baseline distance and the relative frequency bandwidth of the system. The minimum value of baseline for which this term equals zero is the same as that obtained with the conventional critical baseline (B_{nc}) criterion [6].

As it can be seen in Eq. (1), the difference between the two viewing angles produces a shift and a stretch of the imaged terrain spectra in the slant range dimension, which is the cause of the spatial decorrelation. This decorrelation can be compensated by shifting the transmitted center frequency during the second measurement (Tuned Interferometric SAR): $f_{02}/f_{01} = \sin\theta_1/\sin\theta_2$ [1], or by removing the disjoint part of both spectra (which implies a loss of bandwidth and, consequently, resolution).

On the one hand, in wide band interferometry (when the relative bandwidth of the system is very high), the value of B_{nc} becomes very large. From this point of view, we would be able to use long baselines without noticeable loss of correlation. On the other hand, in case the baseline distance is limited by structural aspects of the platform, as in single-pass airborne sensors, the spatial coherence improves as the bandwidth does. Thus, the coherence could reach the maximum value in the wide band case.

However, it has been found experimentally that in wide band measurements there exist other effects which introduce decorrelation (see Section 3). It is shown that the coherence decreases substantially even at short baselines. To explain this coherence loss additional sources of

decorrelation must be identified. One of them, the volumetric effects, appear in the second term of Eq. (6) and indicates a loss of coherence which basically depends on the difference between the two viewing angles and the surface roughness ($\sigma_h{}^2$). This kind of decorrelation also increases as the baseline distance does, but it is negligible in most practical cases. Nevertheless, in principle wide band systems allow the use of large baselines since the spatial decorrelation term is not so important and, therefore, the volumetric decorrelation factor would be more noticeable.

Indeed, the volumetric effects produce a change in the shape of the two imaged terrain spectra and this should be taken into account when B_{nc} is calculated. To this end, if we state that a coherence of $1/e^2(\cong 0.13)$ implies an excessive loss of correlation, from Eq. (6) we can establish a new threshold for the perpendicular critical baseline:

$$B_{nc,vol} = \frac{h}{\pi \cdot \sin(2\theta)} \cdot \frac{\lambda}{\sigma_h} \tag{7}$$

where h is the average height of the antennas. Expression (7) can be used as a tool for designing an operative interferometric system, taking into account the impact of the surface roughness. In this respect, other authors have also presented some effects of the surface parameters on SAR interferometry [7].

As we commented above, it would be possible to eliminate the spatial decorrelation term of Eq. (6) by applying a suitable filter to both spectra. In this way, the effective spectrum of image 1 would be limited to the following range:

$$f_0 - W/2 \leq f \leq (f_0 + W/2)\frac{\sin\theta_2}{\sin\theta_1} \tag{8}$$

while the second spectrum would be between:

$$(f_0 - W/2)\frac{\sin\theta_1}{\sin\theta_2} \leq f \leq f_0 + W/2 \tag{9}$$

Consequently, the center frequencies of both images take the values given by:

$$\begin{aligned} f_{01} &= \frac{f_0}{2}\left(1 + \frac{\sin\theta_2}{\sin\theta_1}\right) - \frac{W}{4}\left(1 - \frac{\sin\theta_2}{\sin\theta_1}\right) \\ f_{02} &= \frac{f_0}{2}\left(1 + \frac{\sin\theta_1}{\sin\theta_2}\right) + \frac{W}{4}\left(1 - \frac{\sin\theta_1}{\sin\theta_2}\right) \end{aligned} \tag{10}$$

If we rewrite Eq. (5) with the new frequencies it is easy to find the new expression:

$$\langle s(\theta_1) \cdot s(\theta_2)^* \rangle \approx C \sum_n \operatorname{sinc}^2(nL \sin\theta / R_s) \cdot \left\langle e^{-j\frac{4\pi}{c} h_n (f_{02}\cos\theta_2 - f_{01}\cos\theta_1)} \right\rangle \tag{11}$$

where the first exponential term, responsible for the spatial decorrelation factor, has been eliminated. In this way, the new coherence equation is only dependent on the volumetric scattering effects:

$$\gamma \approx e^{-2\left(\frac{2\pi}{c}(f_{02}\cos\theta_2 - f_{01}\cos\theta_1)\right)^2 \cdot {\sigma_h}^2} \tag{12}$$

3. SIMULATED AND EXPERIMENTAL RESULTS

Several multifrequency measurements were undertaken in the X-band at the electromagnetic anechoic chamber of the Universitat Politècnica de Catalunya (U.P.C) using the interferometric C-SAR (InCSAR) system [4], whose geometry is illustrated in Figure 2. The C-SAR system allows the antennas to describe a circular trajectory around a rotating mast in order to generate a circular synthetic aperture. They are located at two different heights on the z-axis so as to form a vertical baseline $B = h_2 - h_1$, illuminating the surface at two incidence angles θ_1 and θ_2. The measurement system is basically a vector network analyzer based scatterometer using two closely spaced antennas placed at the end of a 1 meter metallic bar mounted on an azimuth positioner. A personal computer controlled the scatterometer to perform a frequency sweep for each angular sample point. The interferometric measurements comprised a frequency range between 12 and 16 GHz and a baseline range between 0 and 19 cm. For these measurements a metallic flat rough surface was used, with a very low roughness, in the order of a quarter of the wavelength ($\sigma_{hn} = \lambda/4$). Figure 3 shows the interferogram without the flat terrain component corresponding to this surface with a baseline distance of 5 cm. As we can see, it shows a constant phase level close to zero which corresponds to the flat profile of the surface, but there are some zones where the phase of the interferogram is noisy.

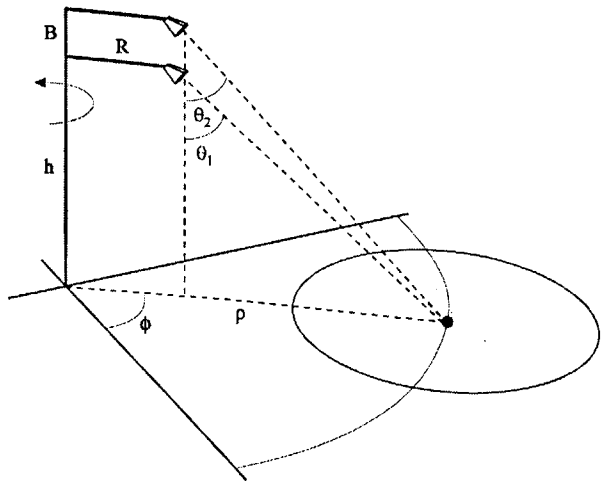

Figure 2. Geometry of the InCSAR system.

Figure 4 shows a comparison between the expected coherence values and those obtained from the experimental results with different baseline distances. The theoretical coherence values are calculated from Eq. (6), neglecting (*) and including (**) the surface roughness, whereas the simulated ones are obtained by numerical computation of the interferometric process from the model described in Eq. (1). As we can see, the theoretical coherence values are very similar to those obtained from the simulation process, which verifies the validity of Eq. (6). However, for longer baselines, the coherence values obtained from the simulation process are lower than those we can predict using the theoretical coherence expression . These differences can be attributed to the approximations assumed in Section 2 regarding the argument of the sinc functions.

An important observation lies in the fact that the coherence values obtained from the experimental results are lower than expected, for the whole range of baselines. After representing the two imaged terrain spectra (Figure 5), it has been found that, in this case, there is not only a frequency shift between the two spectra but also a change in their shape, which implies an important decorrelation and produces a degradation of coherence.

It has also been proved that the coherence can be improved by removing the disjoint parts of the spectra or by implementing a tuned interferometric SAR [1, 5], except for small baseline distances where

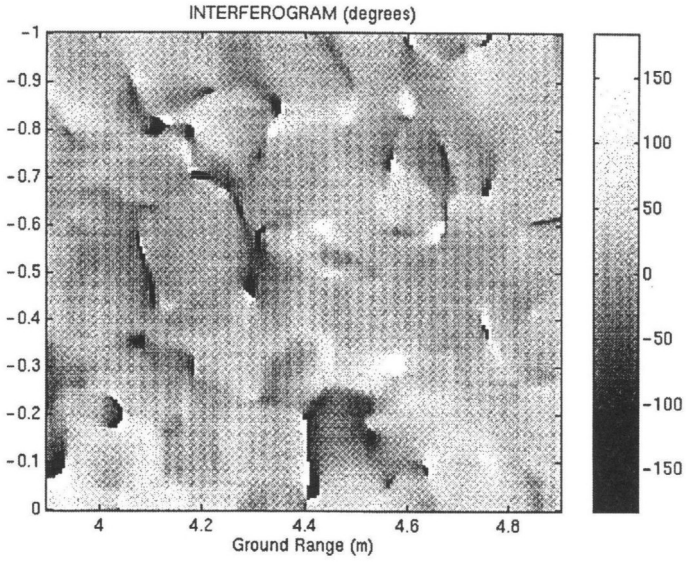

Figure 3. Interferogram without the flat terrain component corresponding to a flat rough surface (B=5 cm).

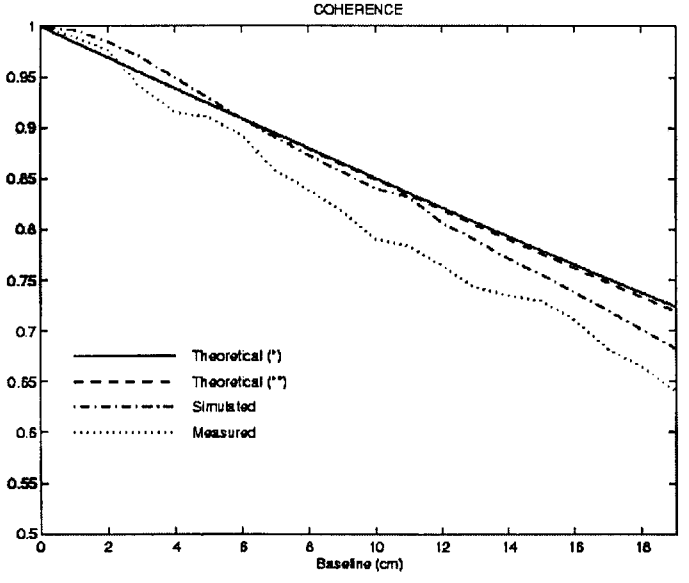

Figure 4. Theoretical (neglecting roughness (*), considering roughness (**)), simulated and measured coherence values corresponding to different baseline distances.

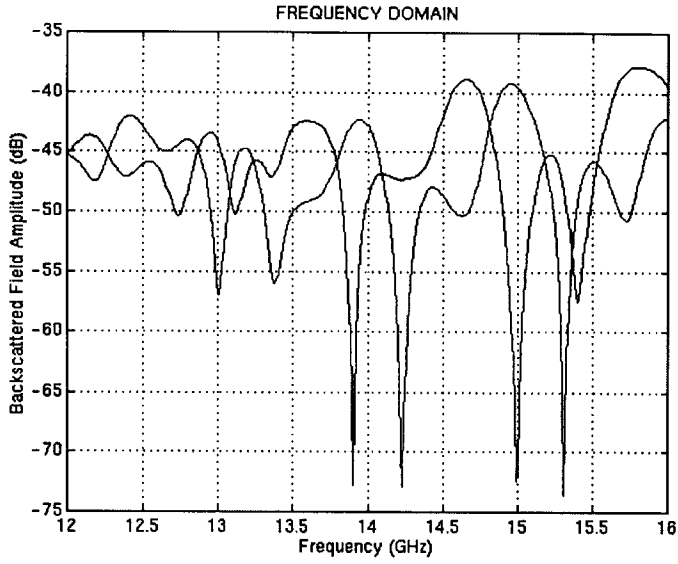

Figure 5. Two imaged surface spectra (B = 5 cm), corresponding to each position of the antennas.

the effect of the spatial term in Eq. (6) can be neglected. Figure 6 shows a cut of each SAR image in the ground range dimension for a baseline distance of 5 cm, comparing the result obtained before and after filtering the non-common parts of the spectra. The interferometric phase derived from the cross-correlation of these two images and their histograms are shown in Figures 7 and 8. As we can see in these figures, the correlation between the two images is higher in the second case and, consequently, the phase error is reduced. Figure 9 shows the obtained coherence values after applying a filter to the disjoint bands. In this case, the spatial decorrelation can be neglected and the coherence is close to 1, as we expected theoretically. In Figure 9 it is possible to notice a slight degradation of the coherence values for long baselines, but this effect can be attributed to a residual effect of the practical implementation of the filtering process, since it is not possible to apply the ideal filter which eliminates completely the non-common parts of the bandwidth. For those baseline values, the approximation of small difference in viewing angles is not completely fulfilled either.

It has been shown that the measured coherence between the two SAR images is improved by removing the spatial decorrelation factor. However, the coherence values obtained from the experimental results

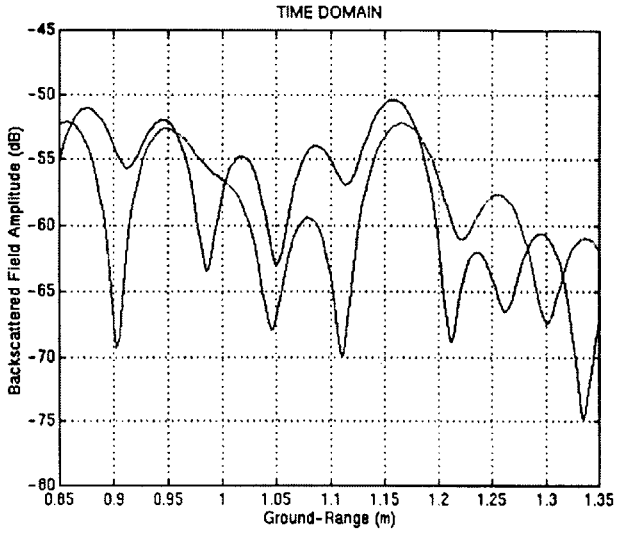

(a)

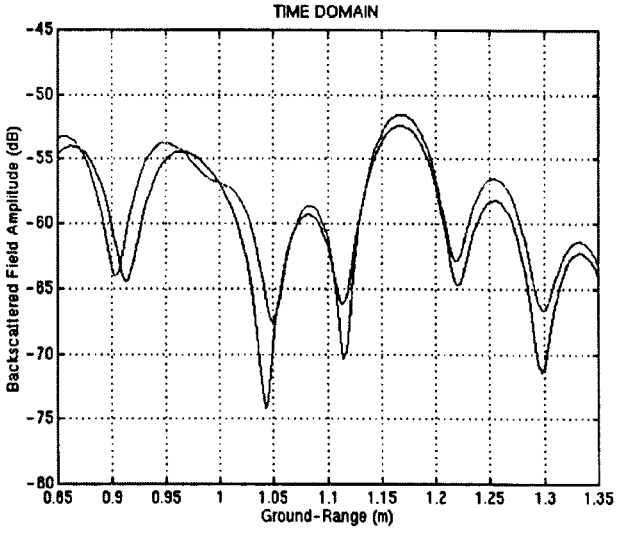

(b)

Figure 6. Cut of the two SAR images in the ground-range dimension, before (left) and after (right) removing the disjoint parts of the spectra.

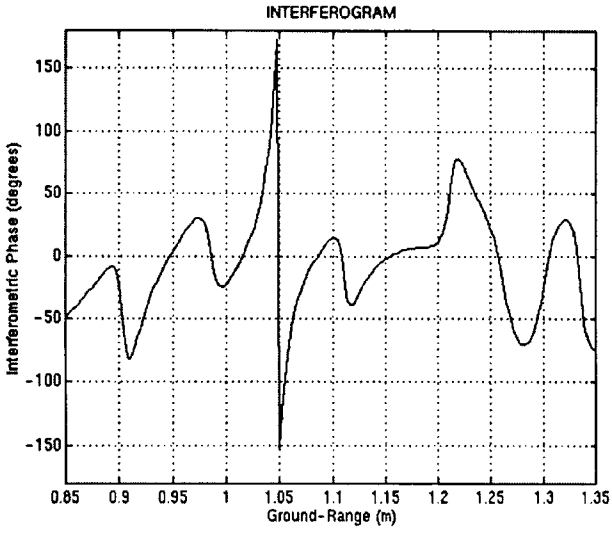

(a)

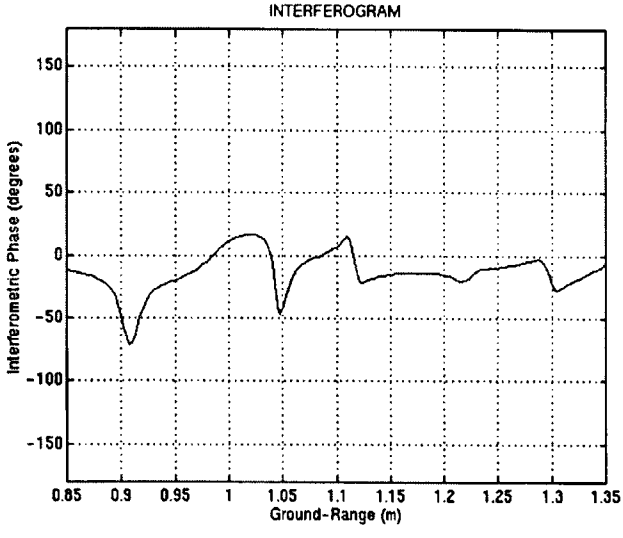

(b)

Figure 7. Interferograms derived from those measurements showed in Figure 6, before (left) and after (right) removing the disjoint parts of the spectra.

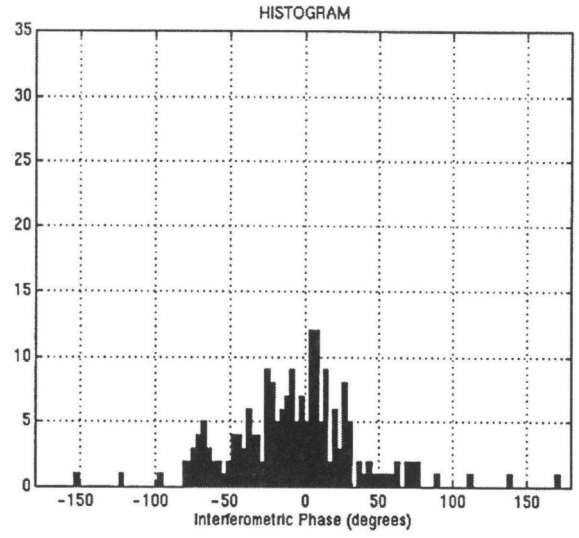

(a)

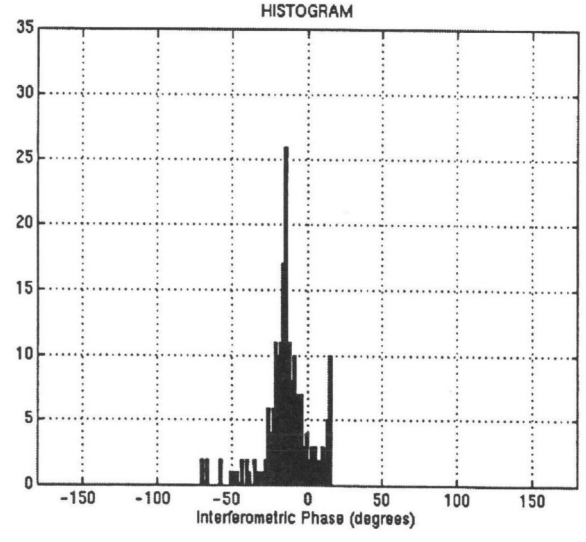

(b)

Figure 8. Interferometric phase histograms corresponding to those interferograms showed in fig. 7, before (left) and after (right) removing the disjoint parts of the spectra.

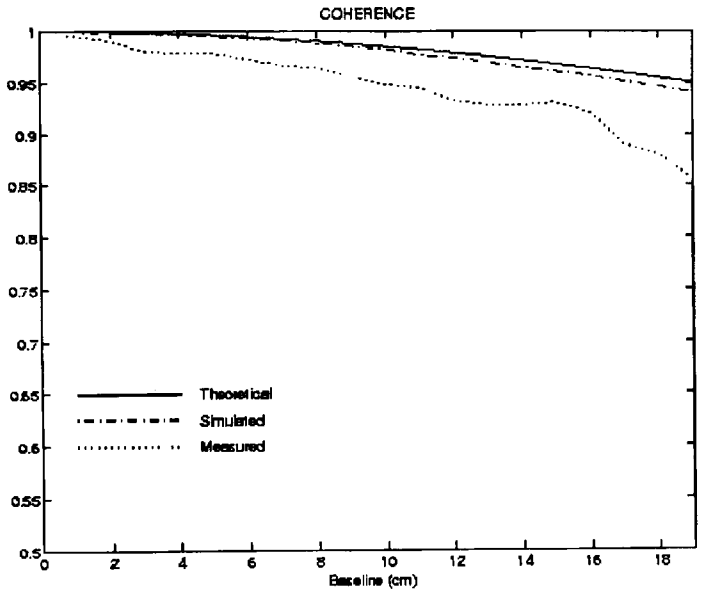

Figure 9. Theoretical, simulated and measured coherence values corresponding to different baseline distances, after removing the disjoint parts of the spectra.

are also lower than expected because of the change of the shape of the two imaged terrain spectra (spectral decorrelation). This change of the spectra becomes very important as the baseline distance increases, which implies that the quality of the interferograms obtained using large baselines can not be substantially improved with the band filtering technique commented above.

Some numerical simulations have been carried out in order to determine the cause of this spectral decorrelation. The results obtained from the simulation process indicate that this change of the spectra shape can not be explained by means of volumetric effects. A different source of decorrelation would be the possible multiple reflections or shadowing phenomena between scatterers, when these effects are different between both antenna positions. It is possible to introduce them in our model by adding or removing some scatterers in one of the two received fields, which would result in a degradation of γ. One exact way to evaluate this interaction between scatterers is the application of the formulation of the method of moments (MoM) [8] for conducting random surfaces. In this way, Figure 10 shows the comparison

between the simulated values of MoM and the experimental ones. As it is displayed, the MoM coherence is in greater accordance with the experiments, what implies that multiple reflection effects are necessary to understand the differences observed with simpler scattering models. Indeed, it would be possible to extend this particular conclusion by affirming that these phenomena are an important source of coherence degradation in a general case.

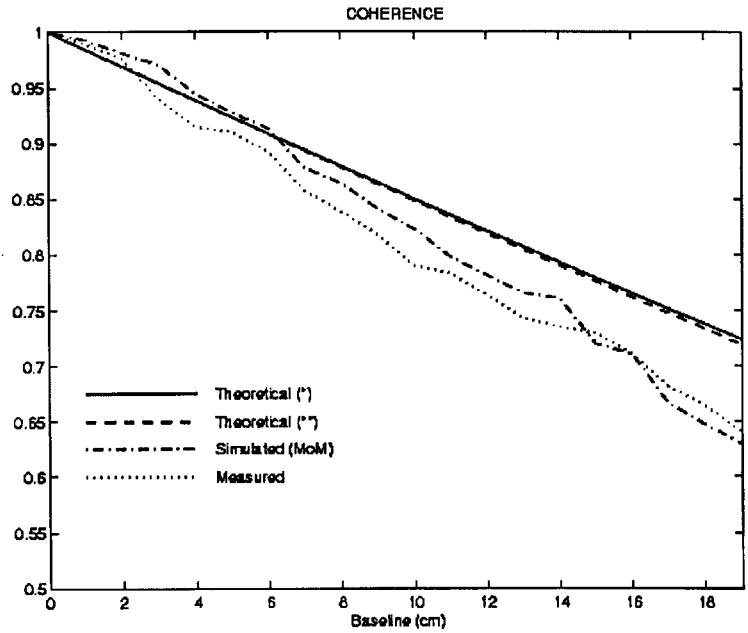

Figure 10. Theoretical (neglecting roughness (*), considering roughness (**)), simulated (applying the method of moments) and measured coherence values corresponding to different baseline distances.

Another explanation of the experimental results, neglected in narrow band interferometry, is the possible variation of the scattering coefficients S_n across the measurement frequency range, due to a different behavior of the surface along the wide bandwidth. Indeed, if we consider that these coefficients are a function of the frequency ($S_n = S_n(f)$), then the resultant coherence would be lower than that of Eq. (6). In this respect, we have developed a model for this frequency variation which is in accordance with the experimental results. Figure 11 shows the coherence values from a simulation process which consid-

ers a sphere frequency behavior for each point scatterer of the surface. As we can see, in this case the coherence is closer to the experimental results. It is worth remarking that this model should be understood as a tool to predict practical coherence values in the wideband case.

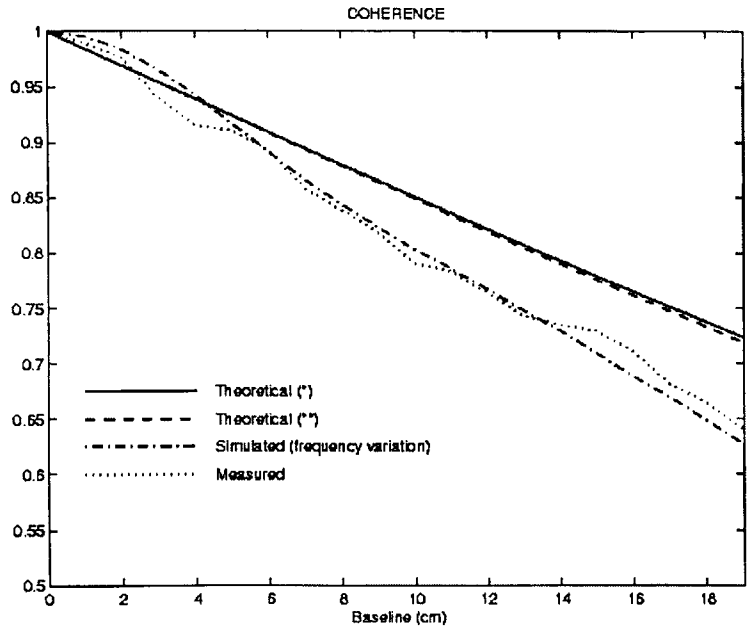

Figure 11. Theoretical (neglecting roughness (*), considering roughness (**)), simulated and measured coherence values corresponding to different baseline distances, when a sphere frequency behaviour is considered for each puntual scatterer.

4. CONCLUSIONS

In this work some experimental results have been presented, with the intention of studying the coherence of interferometric wide band systems. First of all, a model which takes into account the roughness of natural surfaces has been developed. It is considered to describe a metallic rough surface which has been measured in the anechoic chamber of UPC, with different baseline values. Experimental and simulated results are compared, finding that the phase error of the real interferograms is higher than what we can estimate from the conventional phase

standard deviation expression. Even including the surface roughness in the coherence expression, experimental values show that there are other effects related to the wide band which produce an additional decorrelation which does not appear in the narrow band satellite systems. It has been shown by means of numerical simulations that this additional coherence degradation can be produced by two effects: the multiple reflections between scatterers and a frequency variation of the scattering coefficients of the surface along the wide bandwidth. Further work is being carried out to study the evolution of the interferometric coherence as a function of the frequency bandwidth, considering the importance of the scatterers height with regard to the resolution cell size.

ACKNOWLEDGMENT

The authors are grateful for the support from the CICYT (Spanish Commission for Science and Technology) Ref. TIC96–0879, and the CIRIT (Catalan Commission for Research). They also thank reviewers for their suggestions.

REFERENCES

1. Zebker, H. A. and R. M. Goldstein, "Topographic mapping from interferometric synthetic aperture radar obrervations," *Proc. IEEE,* Vol. 62, June 1974.
2. De Porrata, R., A. Broquetas, and X. Fàbregas, "A polarimetric Ultra-Wide band field scatterometer," *IGARSS'95,* Firenze, 1995.
3. Broquetas, A., R. De Porrata, L. Sagués, X. Fàbregas, and Ll. Jofre, "Circular synthetic aperture radar (C-SAR) system for Ground-Based applications," *Electronics Letters,* Vol. 33, No. 11, May 1997.
4. Sagués, L., M. Bara, O. Mora, A. Broquetas, and X. Fàbregas, "Circular synthetic aperture radar (C-SAR) system and an interferometric algorithm for Ground-Based applications," *EUSAR' 98,* Friedrichshafen, 1998.
5. Oh, Y., K. Sarabandi, and F. T. Ulaby, "An empirical model and an inversion technique for radar scattering from bare soil surfaces," *IEEE Transactions on Geoscience and Remote Sensing,* Vol. 30, No. 2, March 1992.

6. Gatelli, F., A. Guarnieri, F. Parizzi, P. Pasquali, C. Prati, and F. Rocca, "The wavenumber shift in SAR interferometry," *IEEE Transactions on Geoscience and Remote Sensing,* Vol. 32, No. 4, July 1994.
7. Sarabandi, K., "Δk-Radar equivalent of interferometric SAR's: A theoretical study for determination of vegetation height," *IEEE Transactions on Geoscience and Remote Sensing,* Vol. 35, No. 5, September 1997.
8. Fung, A. K. and M. F. Chen, "Numerical simulation of scattering from simple and composite random surfaces," *Journal of Optical Society of America,* Vol. 2, No. 12, December 1985.

Lluís Sagués Piella was born in Castellterçol (Barcelona), Spain, in 1972. He received the Diploma degree in Electrical Engineering in 1996 from the Polytechnic University of Catalonia (UPC), Spain, with a thesis on ground-based SAR systems. Since 1996, he has been with the Electromagnetics & Photonics Engineering Group of the Signal Theory & Communications Department of the UPC following a Ph.D. focused on superficial and volumetric scattering analysis of terrains using short radar techniques for SAR and InSAR applications.

Marc Bara Iniesta was born in Barcelona, Spain, in 1972. He received the Diploma degree in Electrical Engineering in 1996 from the Polytechnic University of Catalonia (UPC), Spain, with a thesis on the processing of ERS SAR data. Since 1996, he has been with the Electromagnetics & Photonics Engineering Group of the Signal Theory & Communications Department of the UPC, following a Ph.D. about SAR processing and interferometry focused on motion compensation, geocoding and design of interferometric SAR airborne systems.

Xavier Fàbregas Canovas received the B.S. degree in Physics from the Barcelona University, Spain, in 1988 and the Ph.D. degree in Applied Sciences from the University Polytechnic of Catalonia in 1995. From 1996 he is an Associate Professor at the University Polytechnic of Catalonia. His current research interests include polarimetric retrieval algorithms, polarimetric calibration and polarimetric SAR classification.

Antoni Broquetas Ibars (S'84, M'90) was born in Barcelona, Spain, in 1959. He received the Ingeniero degree in Telecommunication Engineering from the Universitat Politècnica de Catalunya (U.P.C.) in 1985, and the Doctor Ingeniero degree in 1989 in Telecommunications Engineering for his work on microwave tomography in the UPC. In 1986 he was a research assistant in the Portsmouth Polytechnic (U.K.)

involved in propagation studies. In 1987 he joined the Department of Signal Theory and Communications of the School of Telecommunication Engineering of the U.P.C., Barcelona. Currently he is a Professor of the U.P.C. involved in research on radar imaging and remote sensing.